SUBCONTRACT TITLE: **THE FABRICATION AND PHYSICS OF HIGH-EFFICIENCY CADMIUM – TELLURIDE THIN-FILM SOLAR CELLS**

SUBCONTRACT NO: **NDJ-1-30630-02**

QUARTERLY TECHNICAL STATUS REPORT FOR: Phase 3/Quarter 1

SUBMITTED TO: Ken Zweibel
National Renewable Energy Laboratory

PRINCIPAL INVESTIGATORS: A.D. Compaan (P.I.) and V. G. Karpov (co-P.I.)
University of Toledo,
Department of Physics and Astronomy,
2801 W Bancroft,
Toledo, OH 43606

This progress report covers the first quarter of Phase 3 for the period September 01 through November 30, 2003.

The report describes our activities and progress in making CdTe devices by different techniques and understanding their characteristics. More specifically, it describes our recently developed understanding of buffer layer effects, modeling of integrated large-area modules in progress, and our latest efforts in ion implantation (chlorine) and the related changes in photoluminescence (PL).

Buffer-layer-induced reach-through "doping" of CdTe

In comparative studies of buffer layers and back contact doping of CdTe, we have discovered a new physical effect: Schottky barrier suppression in thin-film semiconductors. It occurs through generation of defects that change the semiconductor work function. This translates the effect of metal presence through the semiconductor film and induces a Schottky barrier in another semiconductor tangent to the film on the opposite side (reach-through doping).

More specifically, we consider a three-component system of a thin n-type semiconductor film sandwiched between a metal (or heavily doped transparent conductor) and a p-type semiconductor. In our experimental verification this system is represented by an n-type CdS film between a conductive electrode (TCO) and p-type CdTe. The above system is shown in Fig. 1 (a) for a particular case where the Fermi energies in the film and bulk semiconductor components are close, while being significantly different from that of the metal. Based on the typically observed charge carrier concentration in CdS, we assume that the screening length in CdS is considerably shorter than the film thickness. For such a system, the standard junction theory predicts a weak p-n junction between bulk and thin film semiconductors and a strong Schottky barrier between the metal (TCO) and the film [Fig. 1(b)].

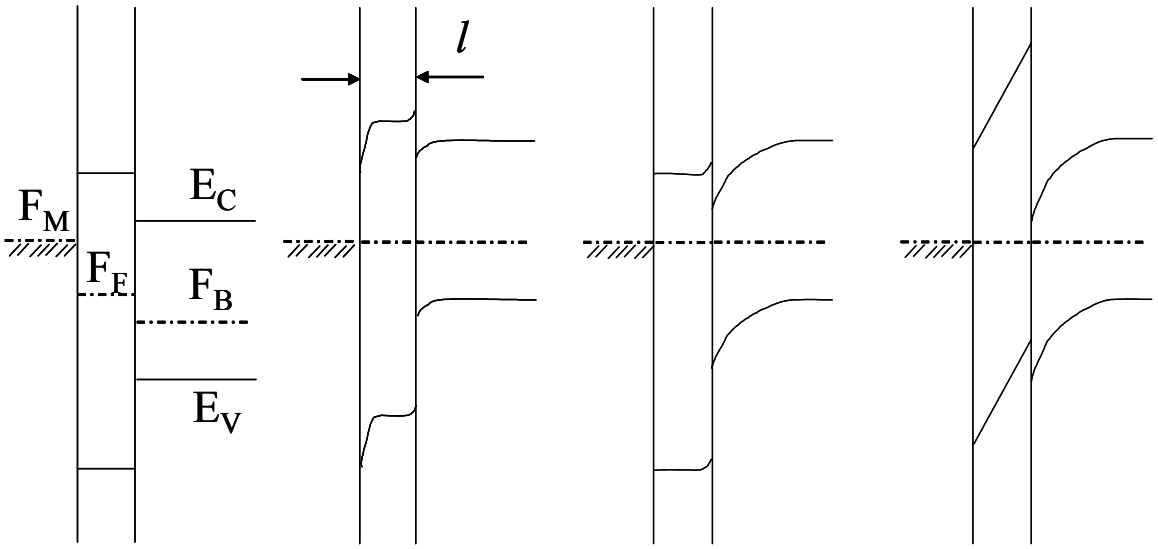

Fig. 1. Energy-band diagrams for a system of metal, semiconductor thin film, bulk semiconductor (not necessarily the same as the thin film) (a) before contact, (b) after contact as predicted by the standard Schottky barrier formation scenario, (c) after contact accompanied by donor defect generation in the thin film, (d) after contact accompanied by acceptor defect generation in the thin film.

Two conceivable effects shown next are due to defect generation: shifting Fermi energy in CdS up [donor-like defects; Fig. 1(c)] and down [acceptor-like defects; Fig. 1(d)]. In the former case, F_F shifts up to F_M; hence, no barrier arises between the metal and the film. It also entails a strong barrier between the semiconductors. In the latter case, the film turns intrinsic, which again makes it possible for the metal to cause a considerable bend bending in the bulk semiconductor across the film similar to MIS structures. In both cases a Schottky barrier appears at the film interface opposite to the metal as though the latter was in direct contact with the bulk semiconductor. This differs significantly from the standard scenario that predicts no effect of the metal presence on the bulk semiconductor.

The experimental verification of the above scenario was based on the understanding that required defects compensating the semiconductor film can be introduced by either chemical doping or through surface states on the interface between the thin film and the metal; we have tried both possibilities. Our experiments were aimed at revealing similarities between the effects of surface modification (via a buffer layer) and doping (Cu diffusion from a back contact). We have measured current-voltage (J-V; Fig. 2), quantum efficiency (QE; Fig. 3) and capacitance-voltage (C-V; Fig. 4).

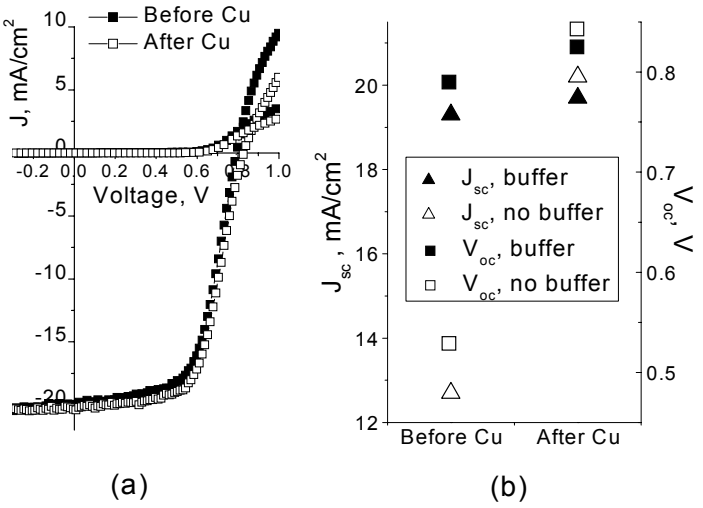

Fig. 2. (a) J-V characteristics of a CdS/CdTe cell containing a 2500 Å thick buffer layer before and after Cu diffusion. (b) Open circuit voltage V_{OC} and short-circuit current J_{SC} for Cu doped and undoped CdS/CdTe structures with and without buffer layer.

Both the open-circuit voltage and short-circuit current (under one-sun light intensity) in Fig. 2 are almost the same in the range of practically significant values for the undoped devices with buffer layer and for doped devices without buffer layer. However, these parameters are much lower and fall in practically unimportant range when neither buffer layer nor Cu doping are present. This shows that either the buffer layer application or Cu doping lead to a well developed junction where the built-in field in the bulk semiconductor (CdTe) is strong enough to provide efficient current collection. Furthermore, close numerical coincidence between the two recipe results suggest that Cu and buffer layer have a similar effect on the CdS layer. Since Cu is known to act as an acceptor in CdS, Fig. 1(d) seems to represent a plausible band diagram for either Cu doped or buffer layer containing structure. This choice is additionally supported by the observation in Fig. 2(a) that the dark J-V curves are abnormally flat thus showing extremely high series resistance that we ascribe to strongly compensated CdS layer (which may become photoconductive). The undoped devices without buffer layer are better described by the diagram in Fig. 1(b), which predicts poorly developed junction and thus low V_{OC} and J_{SC}.

The QE data (Fig. 3) also testify in favor of our interpretation. Since QE represents the number of electron-hole pairs generated per photon, we conclude that carrier collection is equally improved by doping or applying a buffer layer. In addition, the QE of undoped structures without buffer layer are strongly bias-dependent. This means, again in agreement with Fig. 1(b), that the junction is not well developed and thus carrier collection can be considerably improved by reverse bias. Disappearance of such bias dependence after Cu diffusion can be attributed to the formation of a welldeveloped junction. A strong junction consistent with the diagram in Fig. 1(d) is also evident from the QE data for the structures with buffer layer. Similar to the J-V characteristics, the QE remains practically insensitive to Cu doping for structures containing a buffer layer, meaning that the junction, once developed by the buffer layer effect, remains practically insensitive to further material compensation, consistent with our above understanding.

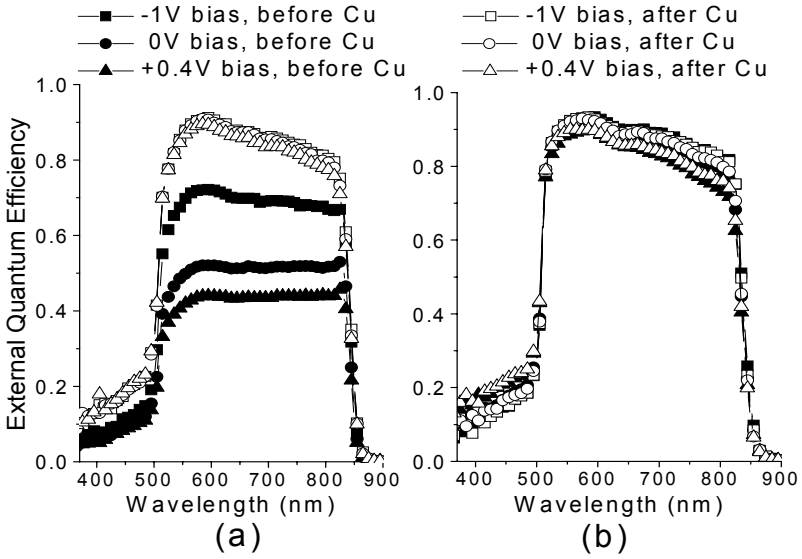

Fig. 3 QE characteristics of CdS/CdTe structures without (a) and with (b) buffer layer for different voltages before and after Cu diffusion.

C-V data (Fig. 4) add specificity to the above interpretation. Samples without buffer layer and Cu show voltage-independent geometrical capacitance. Cu-doping creates a space charge region, which, in accordance with the standard interpretation, is responsible for the slope of 1/C vs. V. [With the J-V in mind, one can assert though that the Cu-related space charge does not contribute much to the device barrier height (close similarity between the Cu and buffer-layer effects)]. Finally, the buffer-layer containing devices exhibit C-V characteristics typical of MIS structures with C varying between two limiting geometrically related values, which again, is consistent with the diagram in Fig. 1(d).

We conclude that the above data confirm the hypothesis of Schottky barrier suppression in the CdS film and show that the metal can act through it causing reach-through doping effects in the bulk CdTe, on the opposite side of the film. Our suggested energy diagram appears to be consistent with the electric field distribution measured in the buffer layer/CdS/CdTe structure by the Kelvin probe technique.[1] Putting it in stronger words, there seems, in most CdS/CdTe cells, to be no p-n junction between CdTe and CdS, but rather a Schottky barrier caused by compensation of the CdS and metal reach-through doping in the CdTe. More generally, our findings suggest that working on the semiconductor thin film can affect the electric field distribution in the bulk semiconductor. One can suggest, for example, that the CdS deposition method (sublimation or sputtering) and temperature will have an effect on the entire device V_{OC}, a prediction that can be verified experimentally.

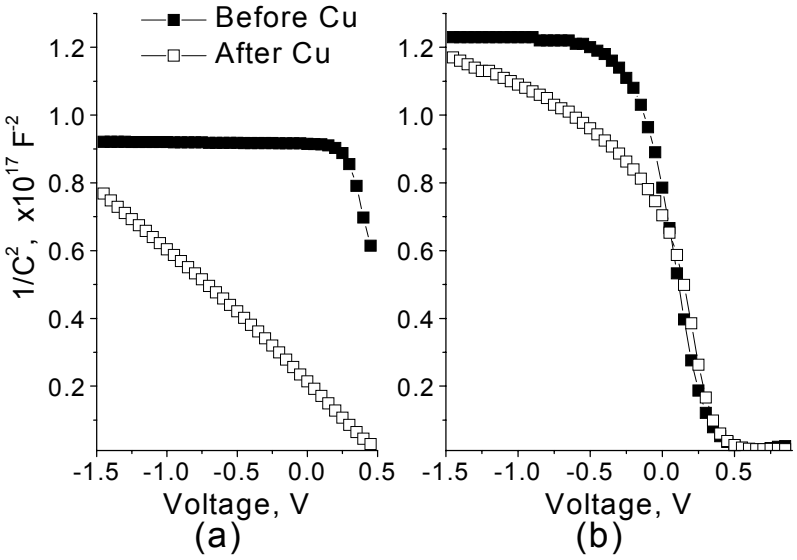

Fig. 4. C-V characteristics of CdS/CdTe structures without (a) and with (b) buffer layer before and after Cu diffusion. In the graph (a) the data are truncated to V<0.5 V to avoid the conduction contribution indicated by the phase angle between the real and imaginary parts of the measured admittance.

Nonuniformity Losses in Large Area CdTe PV modules

We have started numerical modeling of nonuniformity losses in integrated large – area modules. We use PSPICE software modeling that represents an integrated device as a circuit of many photo-diodes with random parameters (Fig. 5). We have preliminary mapped several First Solar devices to collect statistical distributions of their local parameters: Voc, Jsc, Roc, Rsc. To keep the First Solar data proprietary, we then developed numerical techniques to generate the required distributions that are qualitatively similar to the actual data and are flexible enough to allow for any required change in statistical distributions. As an example, shown in Fig. 6 is the Voc distribution. Finally, Fig. 7 shows an example of our modeling results where a nonuniform module efficiency is plotted versus individual cell series resistance.

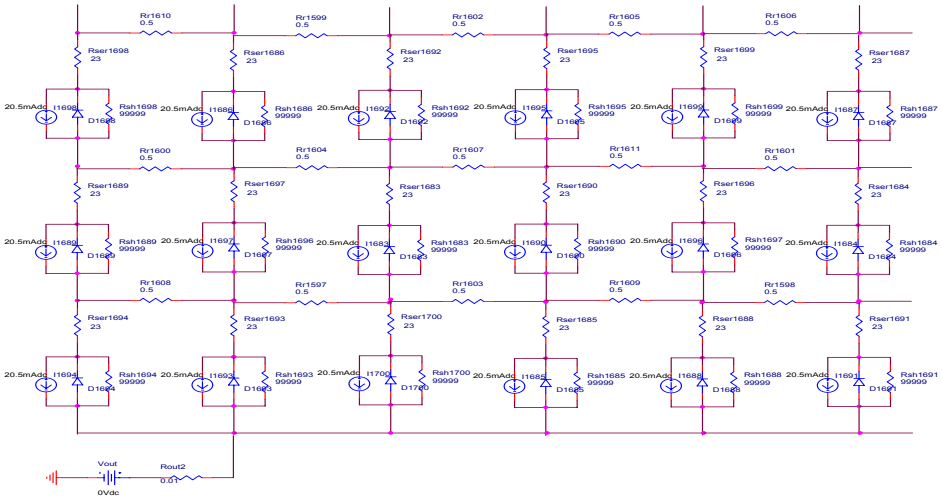

Fig. 5. A fragment of PSPICE model for a nonuniform integrated module consisting of 1682 cells with scribes represented by horizontal conductors, and diodes in parallel with photo-current sources connected with their series resistances along vertical lines.

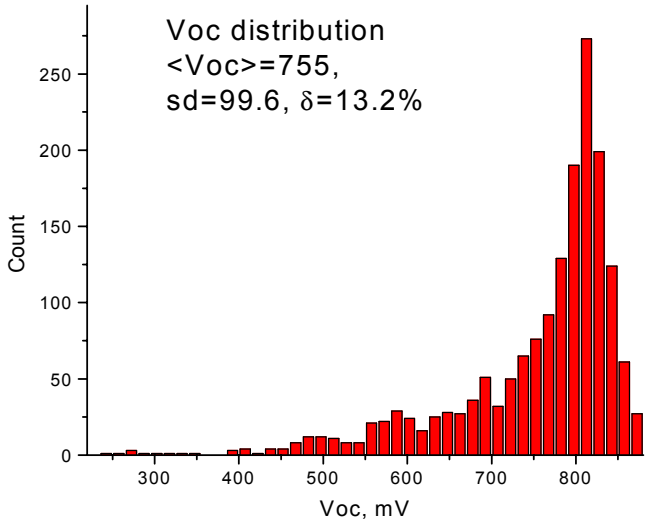

Fig. 6. Histogram of Voc distribution for 1682 individual cells representing an integrated module.

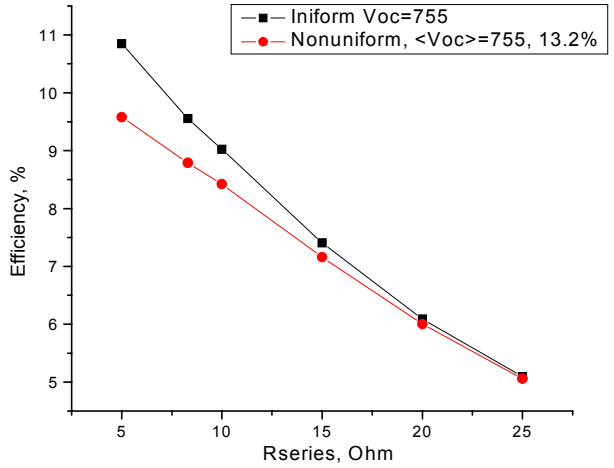

Fig. 7. Integrated module efficiency vs. cell series resistance for uniform and nonuniform modules.

This part of the contract is also in progress. We plan comparison with our (UT) available devices and with a limited available data from First Solar. Also, some published data are available on statistical distributions of PV parameters of nominally identical (same batch) modules that we hope to use for our modeling verification.

Ion implantation and PL studies on high quality crystalline CdTe

We have recently obtained single crystal CdTe from Nikko Materials Co., Ltd, which appears to be higher purity than crystals from Keystone Crystal Co. that we have used in the past. PL on their undoped wafer, Fig. 1, suggests extremely low defect concentration particularly in the deep donor-acceptor level region around 1.39 to 1.44 eV. The phonon-assisted exciton (1.577eV) and bound exciton (1.588~1.592eV) emissions are much stronger than usually observed in wafers from Keystone. In Fig. 8, we show spectra obtained with blue (488 nm) excitation (optical penetration depth $1/\alpha = 0.1$ μm) and with deep red (752 nm) excitation ($1/\alpha = 0.35$ μm), anticipating the need to match optical penetration depth with the ion implnated range.

Because the identification of PL emission lines quickly becomes complicated when there is too great a number of defects, we have chosen to use these samples for ion implantation studies. Ion implantation affords unusual control of the dopant density, particularly when multiple implant energies are used to obtain a flat depth profile. A disadvantage of implantation is the concurrent high damage density. However, our earlier studies have shown that it is possible to anneal this damage using a proximity cap and an inert atmosphere.

It should be noted that there is wafer variability from Nikko. A second wafer from Nikko showed defect features in PL that were similar in intensity to a Keystone crystal, however, it still has stronger exciton and bound exciton emission, as shown in Figure 9.

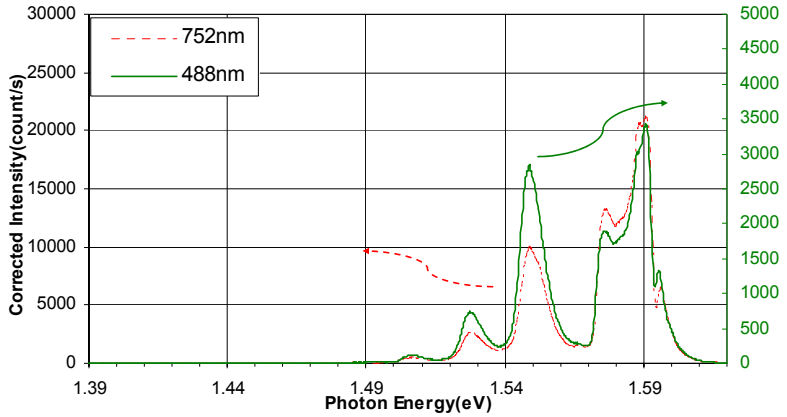

Figure 8. PL on undoped, high quality CdTe wafer from Nikko Materials with two different laser wavelengths at a power density equivalent to 350 suns (35 W/cm^2).

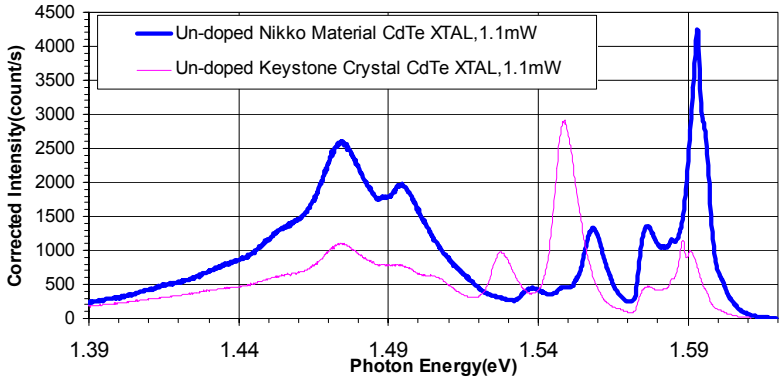

Figure 9. PL on a second quality CdTe wafer from Nikko Materials and from Keystone Crystal, excited at 752nm with intensity of 100 suns (10 W/cm^2).

We have studied Cl implants and a variety of other species. The implantation was done through collaboration with the atomic physics group at the University of Toledo on the accelerator in the Physics and Astronomy Department. The Cl^{++} and Cl^{+} ions were implanted into the second quality CdTe wafer from Nikko Materials Co., at three different energies: 400, 200 and 100 keV with total doses of $1.17x10^{10}$, $3.9x10^{10}$ and $3.9x10^{11}$, $3.9x10^{12}$ /cm^2 to yield, respectively, implanted Cl densities of $3x10^{16}$, $1x10^{17}$, $1x10^{18}$, $1x10^{19}$ Cl/cm^3. The total doses were split 72%/19%/9%, respectively, at the energies of 400, 200 and 100 keV, to give uniform implanted Cl densities. The projected range and range straggling are, respectively, 0.264 and 0.143 μm calculated from the Monte Carlo program "SRIM"--- The Stopping and Range of Ions in Matter. These energies were chosen to match the absorption length of the 752 nm PL excitation laser (0.35μm) and obtain a smooth ion distribution. Annealing at 400 ^{o}C in N_2 for 30 minutes, with the implanted side of the crystal face down on a sputtered CdTe film (proximity cap), was done to remove most of the vacancies and interstitials produced by the implantation.

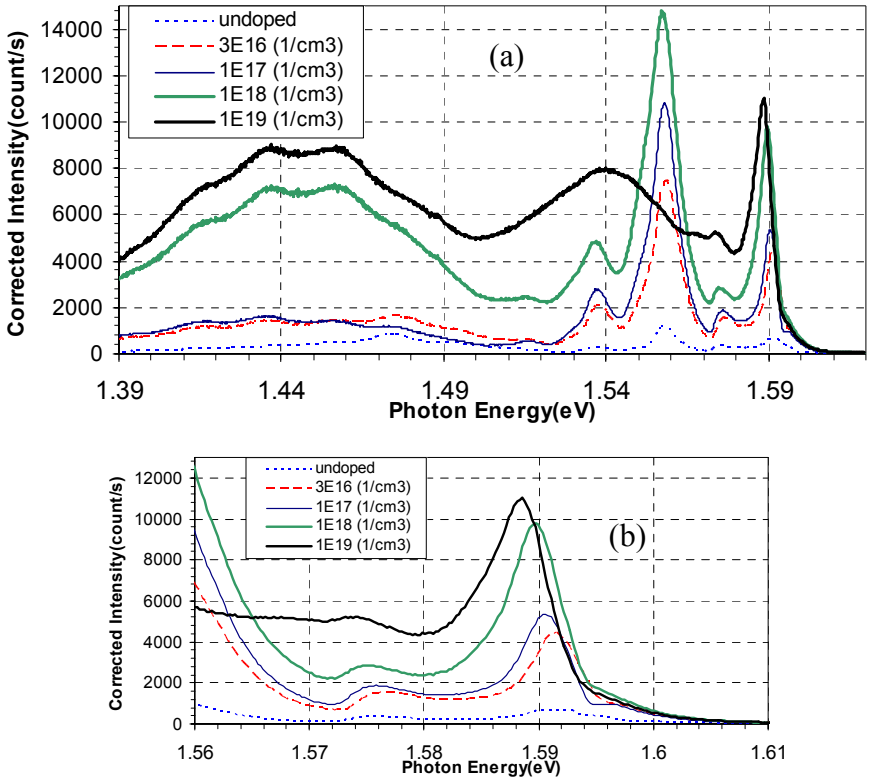

Figure 10. PL from an annealed, Cl-implanted CdTe wafer from Nikko Materials, excited at 752nm with intensity of 37 suns: a) full spectrum; b) expanded display of the acceptor-bound excition feature (A^oX) showing the shift to lower energy as Cl dopant density increases.

Photoluminescence was studied both before and after annealing. The post-annealing spectra are presented in Figure 10 for an intermediate laser poser. The intensities of most features in the spectra increase with Cl dopant concentration. These include the deep donor-acceptor pair band, free exciton and band-to-band, and the bound exciton emission. The broad band at 1.54 eV in the spectrum of the wafer implanted with $1x10^{19}$ /cm^3 Cl, is probably related to insufficient annealing. We think this may be a consequence of the higher dose producing a fully amorphous top layer which then is much more difficult to recrystallize than layers with lower dose. The A^oX predominates in the bound exciton emissions and shifts to lower energy as the Cl concentration increases (Figure 10b).

Deconvolution of peaks is in progress as well as analysis of the excitation power dependence to understand the origin of individual emission lines. Due to having only a small amount of the higher quality wafer supplied by NM, we only prepared one Cl-implanted sample with a Cl implant dose of $1.17x10^{10}$ /cm^2. We plan to present PL on this sample at the coming Team meeting at Toledo, OH.

[1] I. Visoly-Fisher, S. R. Cohen, and D. Cohen, Appl. Phys. Lett. **83**, 4924 (2003)